Journal of Translational Medicine

RESEARCH

Open Access

SULF1 expression is increased and promotes fibrosis through the TGF-β1/SMAD pathway in idiopathic pulmonary fibrosis

Meng Tu[1,2], Chunya Lu[1,2], Hongxia Jia[1], Shanshan Chen[1,2], Yan Wang[1], Jing Li[1], Jiuling Cheng[1], Ming Yang[3,4*] and Guojun Zhang[1,2*]

Abstract

Background Idiopathic pulmonary fibrosis (IPF) is a chronic and progressive interstitial lung disease of unknown etiology. Despite the increasing global incidence and poor prognosis, the exact pathogenic mechanisms remain elusive. Currently, effective therapeutic targets and treatment methods for this disease are still lacking. This study tried to explore the pathogenic mechanisms of IPF. We found elevated expression of SULF1 in lung tissues of IPF patients compared to normal control lung tissues. SULF1 is an enzyme that modifies heparan sulfate chains of heparan sulfate proteoglycans, playing a critical role in biological regulation. However, the effect of SULF1 in pulmonary fibrosis remains incompletely understood. Our study aimed to investigate the impact and mechanisms of SULF1 in fibrosis.

Methods We collected lung specimens from IPF patients for transcriptome sequencing. Validation of SULF1 expression in IPF patients was performed using Western blotting and RT-qPCR on lung tissues. ELISA experiments were employed to detect SULF1 concentrations in IPF patient plasma and TGF-β1 levels in cell culture supernatants. We used lentiviral delivery of SULF1 shRNA to knock down SULF1 in HFL1 cells, evaluating its effects on fibroblast secretion, activation, proliferation, migration, and invasion capabilities. Furthermore, we employed Co-Immunoprecipitation (Co-IP) to investigate the regulatory mechanisms involved.

Results Through bioinformatic analysis of IPF transcriptomic sequencing data (HTIPF) and datasets GSE24206, and GSE53845, we identified SULF1 may potentially play a crucial role in IPF. Subsequently, we verified that SULF1 was upregulated in IPF and predominantly increased in fibroblasts. Furthermore, SULF1 expression was induced in HFL1 cells following exposure to TGF-β1. Knockdown of SULF1 suppressed fibroblast secretion, activation, proliferation, migration, and invasion under both TGF-β1-driven and non-TGF-β1-driven conditions. We found that SULF1 catalyzes the release of TGF-β1 bound to TGFβRIII, thereby activating the TGF-β1/SMAD pathway to promote fibrosis. Additionally, TGF-β1 induces SULF1 expression through the TGF-β1/SMAD pathway, suggesting a potential positive feedback loop between SULF1 and the TGF-β1/SMAD pathway.

Conclusions Our findings reveal that SULF1 promotes fibrosis through the TGF-β1/SMAD pathway in pulmonary fibrosis. Targeting SULF1 may offer a promising therapeutic strategy against IPF.

Keywords Idiopathic pulmonary fibrosis, SULF1, TGF-β1, Fibroblasts, TGF-β1/SMAD pathway

*Correspondence:
Ming Yang
Ming.Yang@newcastle.edu.au
Guojun Zhang
zgj@zzu.edu.cn
Full list of author information is available at the end of the article

Introduction

Idiopathic pulmonary fibrosis (IPF) is a chronic and progressive interstitial lung disease (ILD) of unknown etiology characterized by excessive differentiation and proliferation of myofibroblasts, progressive deposition of extracellular matrix (ECM), and histological and radiological features consistent with usual interstitial pneumonia (UIP). It is associated with worsening respiratory symptoms, declining lung function, and ultimately fatal outcomes [1, 2]. IPF tends to occur in middle-aged and elderly people, with a global incidence estimated at 0.09–1.30 per 10,000 individuals, increasing annually. Adjusted rates in the Asia–Pacific region range from 0.35 to 1.30 per 10,000, with prevalence estimates ranging from 0.57 to 4.51 per 10,000 and showing an upward trend [3, 4]. The prognosis of IPF is poor, with 1, 2, and 5-year survival rates of 61%, 52%, and 39%, respectively [5].

The pathogenesis of IPF is believed to involve complex interactions among various cell types and signaling pathways, although specific mechanisms remain unclear [6–8]. Currently, two anti-fibrotic drugs, pirfenidone and nintedanib, are approved for IPF treatment, aimed at reducing the decline in lung function [9, 10]. Non-pharmacological approaches such as pulmonary rehabilitation, palliative care, management of comorbidities, and acute exacerbations have also been explored to improve symptom control and quality of life. Lung transplantation remains the only effective therapeutic option for end-stage IPF. Unfortunately, to date, effective therapeutic targets and curative internal medicine methods for IPF are still lacking [11]. As a fatal pulmonary disease, the survival rate of IPF is poorer compared to many malignant tumors affecting similar demographic groups [12].

In this study, we collected IPF lung tissue specimens for transcriptome sequencing and integrated publicly available IPF lung tissue transcriptomic data from the GEO database. We identified elevated expression of Sulfatase 1(SULF1) gene in IPF patients. SULF1 gene, located on 8q13.2-q13.3, encodes an extracellular heparan sulfate endosulfatase, which selectively removes 6-O-sulfate groups from the heparan sulfate chains of heparan sulfate proteoglycans (HSPGs), a crucial process in biological regulation [13, 14]. HSPG can bind to various protein ligands, including growth factors, growth factor receptors, formatin, cytokines, chemokines, proteases, and esterases [15]. Analysis of single-cell sequencing data from IPF patients further revealed high SULF1 expression in fibroblasts. Fibroblast foci are a hallmark of IPF pathology, comprising abnormally activated fibroblasts and myofibroblasts. These cells, when stimulated under various pro-fibrotic conditions, play a critical role in driving ECM deposition. Furthermore, sustained myofibroblast phenotypes contribute to impaired lung repair, tissue scarring, distortion of alveolar structures, and irreversible decline in lung function [16, 17]. Hence, SULF1 may play a crucial role in the initiation and progression of IPF.

Materials and methods

Lung tissue and blood

This study enrolled 8 patients with IPF who underwent lung transplantation surgery at the First Affiliated Hospital of Zhengzhou University from August 2021 to August 2023, along with adjacent normal lung tissues from 8 patients undergoing surgery for benign lung nodules, all stored in liquid nitrogen. Additionally, peripheral venous blood samples (3 ml) were collected from 20 IPF patients and 20 healthy individuals undergoing routine health check-ups during the same period.

RNA sequencing

RNA sequencing analysis was performed on 8 samples of IPF lung specimens and 4 adjacent healthy lung tissues from benign pulmonary nodules surgery (Human Tissue-IPF dataset, HTIPF), with sufficient sample sizes collected. TRIzol (Invitrogen, USA) was utilized for the extraction of total RNA from lung tissue samples of IPF patients. RNA integrity was assessed using the RNA Nano 6000 Assay Kit of the Bioanalyzer 2100 system (Agilent Technologies, CA, USA). Total RNA underwent library preparation, beginning with mRNA purification and fragmentation. The resulting fragments were used to synthesize first and second-strand cDNA, with blunt ends generated afterward. Adapters were then ligated to facilitate hybridization, and fragments of 370–420 bp were selectively purified. PCR amplification was conducted, and the resulting products were assessed for quality. Subsequently, clustering of samples was carried out using the TruSeq PE Cluster Kit v3-cBot-HS (Illumia) on a cBot Cluster Generation System, followed by sequencing on an Illumina Novaseq platform to generate 150 bp paired-end reads.

GEO data collection

The datasets GSE24206, GSE53845, GSE110147, and GSE122960 were downloaded from the Gene Expression Omnibus (GEO, http://www.ncbi.nlm.nih.gov/geo) database. GSE24206 includes 23 lung tissue samples from 6 healthy subjects and 11 patients with IPF. Among the IPF patients, 5 donated single samples, while 6 individuals contributed paired samples from both upper and lower lung lobes. GSE53845 includes 48 lung tissue samples from 40 IPF patients and 8 healthy controls. GSE110147 includes 48 lung tissue samples from 22 IPF, 10 NSIP and 5 mixed IPF-NSIP, and 11 healthy patients. GSE122960 includes Single-cell RNA sequencing (scRNA-seq) data

of lung tissues from 8 donors and 9 patients with diverse forms of pulmonary fibrosis. We selected data from 4 IPF patients and 8 healthy donors for analysis.

Identification of differentially expressed genes (DEGs)

The data was standardized and corrected through the limma package of R (4.3.3). Differential analysis between IPF and Control groups was performed separately on the GSE24206 and GSE53845 datasets using the limma package. The criteria of DEGs was |log2 fold change (FC)| > 1.5 and adjusted $P < 0.05$. After this, according to the positive and negative value of FC, genes were divided into up- and down-regulated genes, Venn diagrams were generated using package ggplot 2(3.3.6) and VennDiagram (1.7.3) to identify genes commonly altered between the two datasets.

Construction of PPI network and module analysis

The Search Tool for the Retrieval of Interacting Genes (STRING) is an online tool that assesses protein–protein interaction (PPI) network information. STRING (version 12.0) was used to evaluate the potential PPI relationships among those DEGs. Only experimentally validated interactions with a combined score ≥ 0.4 were selected as significance. The PPI network was constructed and visualized using Cytoscape software (3.9.1). The molecular complex detection (MCODE) plug-in in Cytoscape was used to screen the modules of the PPI network. Subsequently, 12 sets of top 10 genes were generated from 12 topological analysis methods (BottleNeck, Closeness, Degree, DMNC, EcCentricity, EPC, MCC, MNC, Radiality, Betweenness, Stress, ClusteringCoefficient) of CytoHubba, The UpSet plot was generated using package ggplot 2 (3.3.6) to elucidate the distribution patterns of the 12 sets of top 10 genes.

scRNA-seq data analysis

Using R (version 4.3.3) and the Seurat package, the dataset GSE122960 was processed and analyzed. Following data preprocessing and quality control, the following detailed steps were undertaken: (1) Standardization of samples using the SCTransform function; (2) Principal Component Analysis (PCA) using the RunPCA function; (3) Calculation of cell similarity using the FindNeighbors function with mutual nearest neighbor (MNN) algorithm; (4) Spatial clustering of cells based on the nearest neighbor distance matrix using the FindClusters function; (5) Visualization of data in two-dimensional space using the RunUMAP function; (6) Annotation of cell types by marking the expression of various cell marker genes using the FeaturePlot function. UMAP plots, violin plots, and bubble plots were generated using Seurat package. The SplitObject function was used to partition Seurat objects into multiple subsets by samples. For each subset, gene expression data was extracted using the GetAssayData function, and the correlation between the expression levels of TGFBR3 and SULF1 was calculated. Statistical testing was performed using the Wilcoxon rank-sum test, with $P < 0.05$ considered statistically significant.

Cell culture and treatments

The human fetal lung fibroblast cell lines MRC-5 and HFL1 were obtained from Wuhan Procell Life Science and Technology Co. Ltd. (Wuhan, China).

MRC-5 was cultured in MEM medium supplemented with 10% fetal bovine serum and 1% penicillin–streptomycin. HFL1 cells are cultured in Ham's F-12K medium supplemented with 10% fetal bovine serum and 1% penicillin–streptomycin. All cell lines were grown in a 5% CO2 condition at 37 ℃. Treatment with recombinant human TGF-β1 (10 ng/ml, PeproTech, USA) for 48 h in a medium containing 1% FBS was employed to induce the activation and transformation of fibroblasts into myofibroblasts. SIS3 is a selective Smad3 inhibitor, that can attenuate TGF-β1-dependent Smad3 phosphorylation. Treatment of cells with SIS3 dissolved in DMSO (Solarbio, China) at a concentration of 10 μM, along with 10 ng/ml concentration of TGF-β1, was conducted for 48 h. The control group received an equivalent volume of DMSO.

Enzyme-linked immunosorbent assay (Elisa)

The concentration of SULF1 in plasma was measured according to the manufacturer's protocol in the Human Extracellular Sulfatase Sulf1 (SULF1) ELISA kit (Cusabio, China). To eliminate the influence of TGF-β1 in fetal bovine serum, HFL1 cells were cultured in serum-free basal medium. Cell culture supernatants were collected at 0 h, 24 h, and 48 h, centrifuged at 500*g* for 5 min to remove debris, and stored at −80 °C. The TGF-β1 content in the cell culture supernatant was measured following the manufacturer's protocol in the Human TGF-beta1 ELISA kit (Proteintech, China).

RNA extraction and Real-time quantitative reverse transcription PCR (RT-qPCR)

Total RNA was extracted using Trizol (15596026, Invitrogen, USA) according to the manufacturer's instructions. The total RNA was reverse transcribed into cDNA using the RevertAid First Strand cDNA Synthesis Kit (K1622, Thermo, USA). Subsequently, RT-qPCR was performed following the manufacturer's protocol of Maxima SYBR Green qPCR Master Mix (2×) (K0251, Thermo, USA). The RT-qPCR was carried out on a PCR device (Applied Biosystems: 7500, Thermo Fisher Scientific).

The expression levels of the target genes were normalized using GAPDH as a reference. Relative gene expression was determined using the $2^{-\Delta\Delta Ct}$ method, and all results are presented as the mean of three replicates. The primer sequences are shown in Table S1 of Supplementary Material.

Western blotting

Total protein from cells and tissues was extracted using RIPA lysis buffer (Servicebio, Wuhan, China) supplemented with a 100:1 ratio of phosphatase inhibitor (Servicebio, Wuhan, China) and PMSF (Servicebio, Wuhan, China). The protein concentration was determined using the Omni-Easy Instant BCA Protein Assay Kit (EpiZyme, Shanghai, China). Subsequently, the total protein was diluted with 5×SDS-PAGE loading buffer (Servicebio, Wuhan, China) in a 4:1 ratio and boiled at 100 °C for 5 min. The proteins were separated by SDS-PAGE Gel electrophoresis and transferred onto a PVDF membrane. The membrane was blocked with blocking buffer (EpiZyme, Shanghai, China) and then incubated with primary antibodies against SULF1 (1:1000, A13797, ABclonal), SMAD2 (1:1000,#5339, CST), Phospho-SMAD2 (1:1000,#18338, CST), SMAD3 (1:1000,#9523, CST), Phospho-SMAD3 (1:1000, #9520, CST), COL1A1 (1:1000, #72026, CST), α-SMA (1:1000, #19245, CST), FN1 (1:1000, ab2413, Abcam), DESMIN (1:1000, ab32362, Abcam), and β-ACTIN (1:1000, GB15003, Servicebio, China), as well as TGF-β1 (1:1000, Bioss, bsm-33287M). After incubation overnight at 4 °C, the membrane was further incubated with HRP Goat Anti-Rabbit IgG (1:10,000, H6162, UElandy) or HRP Goat Anti-Mouse IgG (1:10,000, H6161, UElandy), at room temperature for 1 h. Finally, the PVDF membrane was covered with enhanced chemiluminescence reagents (SQ201, EpiZyme) and the image was captured using the GE Amersham Imager 680 image analysis equipment. The grayscale intensities of the bands were evaluated using Image J version 1.53.

Cell transfection

The lentiviruses carrying SULF1 shRNA (sh-SULF1: GCACCAAATATGGATAAACAC) and control sequences (sh-NC: TTCTCCGAACGTGTCACGT) were obtained from Jikai Gene Technology (Shanghai, China). To establish stable transfected cell lines, HFL1 cells were seeded at a density of 3.0×10^5 cells/well in 6-well plates. When the cell growth density reached 30%, they were transfected with an MOI of 10 for 10 h and then the medium was replaced with fresh culture medium. Transfected cells were cultured in puromycin (2 μg/ml, Servicebio, China) for 7 days to establish a stable transfected cell line.

Wound-healing assay

The cells were seeded at a density of 5.0×10^5 cells/well in 6-well plates. When the cell growth density reached 100%, a 200 μl pipette tip was used to create a scratch perpendicular to the bottom of the 6-well plate, followed by washing three times with phosphate-buffered saline (Servicebio, Wuhan, China). Serum-free culture medium was added to continue cultivation. Cell conditions were observed and photographed every 12 h. The migration area (%) was evaluated using the formula: The migration area (%) = $(A0-An)/A0\times100$, where A0 represents the initial scratch area and An represents the scratch area at the termination of observation. The area of the scratch was measured using Image J version 1.53.

Cell counting kit-8 (CCK-8) assay

Cells were seeded in 96-well plates at a density of 6000 cells/well. At 0, 24, 48, and 72 h post-seeding, 10 μl of CCK-8 solution (Dojindo, Tokyo, Japan) was added to each well. Following a 2-h incubation at 37 °C, the optical density (OD) value was measured at 450 nm wavelength using a microplate reader (SpectraMax i3x, Molecular Devices, USA). GraphPad Prism (Version 9.3.1) was utilized for plotting the proliferation curves.

5-Ethynyl-2′-deoxyuridine (EdU) assay

The EdU assay was conducted using the BeyoClick™ EdU Cell Proliferation Kit with Alexa Fluor 594 (Beyotime, Shanghai, China). Briefly, cells were seeded in 96-well plates at a density of 2.5×10^4 cells/well and cultured overnight. Then, cells were washed with PBS and incubated with fresh culture medium containing 10 μM EdU for an additional 2 h at 37 °C. Subsequently, cells were fixed with 4% paraformaldehyde and stained with Hoechst 33342 solution to visualize cell nuclei. Images were acquired using a fluorescence microscope (Olympus IX73). The proportion of EdU-positive cells was quantified using Image J version 1.53.

Transwell invasion assay

For the transwell invasion assay, Matrigel (356234, BD Biosciences, USA) was diluted to 300 μg/ml in basal culture medium and applied to the upper surface of Transwell chamber (Corning Costar, USA) membranes. The coated chambers were then incubated at 37 °C for 3 h. In the lower chamber, 700 μl of cell culture medium containing 20% serum was added. A total of 100 μl of serum-free Ham's F-12K medium containing 5×10^4 cells was placed in the upper chamber of a 24-well Transwell plate. After 48 h of incubation at 37 °C with 5% CO2, the invaded cells were fixed with 4% paraformaldehyde (Leagene Biotechnology, China) and stained with 0.1%

crystal violet (Leagene Biotechnology, China), while non-invaded cells were removed using a cotton swab. The number of invaded cells was manually counted in three randomly selected areas under a fluorescence microscope (Olympus IX73).

Co-immunoprecipitation (Co-IP)

HFL1 cells were treated with TGF-β1 for 48 h, followed by lysis using Co-IP lysis buffer (87787, Thermo Scientific). Co-IP was performed using anti-TGFβRIII antibody (#5544, CST) and Protein A/G magnetic beads (B23201, Bimake) according to the manufacturer's protocol. The immunoprecipitated samples were subjected to Western blotting analysis using antibodies against SULF1 and TGF-β1.

Statistical analysis

All statistical analyses were performed using GraphPad Prism (Version 9.3.1). The data were presented as the mean with the standard error of the mean (SEM) from at least three independent experiments. Student's t-tests were employed to compare differences between two groups, while one-way ANOVA was utilized for comparisons involving more than two groups. Two-way ANOVA was utilized for the analysis of variance with 2 factors. All statistical tests were two-sided and $P < 0.05$ was considered to be statistically significant.

Result

SULF1 was upregulated in IPF

We integrated our self-test transcriptome sequencing dataset HTIPF with datasets GSE24206 and GSE53845 to compare DEGs between lung tissues of IPF patients and healthy controls. A total of 23 upregulated and 6 downregulated genes were identified across the three datasets (Fig. 1A). Using Cytoscape software with the MCODE plugin, we identified 17 hub genes and applied CytoHubba plugin with 12 topological methods to analyze the distribution of the top 10 genes. Ultimately, we selected 5 core genes: COL1A1, COL15A1, COL10A1, SULF1, and CTHRC1 (Fig. 1B, C). Further validation in the GSE110147 dataset confirmed higher expression of these 5 genes in IPF compared to normal controls ($P < 0.001$). Validation experiments showed that SULF1 expression in IPF patient lung tissues was significantly higher than in normal controls at both mRNA and protein levels ($n = 8$, $P < 0.001$; Fig. 1E, F). Additionally, plasma levels of SULF1 were elevated in IPF patients compared to healthy individuals ($n = 20$, $P < 0.001$; Fig. 1G). These findings indicate elevated expression of SULF1 in both lung tissues and plasma of IPF patients compared to healthy controls.

SULF1 was upregulated in human lung fibroblasts

Single-cell transcriptomic dataset GSE122960 from IPF lung tissues was utilized to analyze the expression pattern of SULF1 in various lung cell types. Figure 2A provides cell type annotations, while Fig. 2B illustrates the distribution of cells from IPF and healthy control patients in different cell clusters. Subsequent analysis of SULF1 expression levels across individual cell populations revealed higher expression in IPF patients compared to healthy controls, with fibroblasts from IPF patients showing the highest expression (Fig. 2C). Given the important role of fibroblasts in the pathogenesis of pulmonary fibrosis, human lung fibroblasts were selected for further investigation.

SULF1 expression was induced in human pulmonary fibroblasts after exposure to TGF-β1

We selected human lung fibroblast cell lines HFL1 and MRC-5 for cellular experiments. Upon stimulation with TGF-β1, mRNA levels of SULF1 gradually increased over time in both HFL1 and MRC-5 cells, with significant elevations observed at 48 h compared to the Blank group (all $P < 0.05$, Fig. 3A, B). Activation markers of fibroblasts, including ACTA2 and DESMIN, as well as mRNA levels of ECM components such as COL1A1 and FN1, also showed a similar increasing trend over time and were significantly higher at 48 h stimulated by TGF-β1 (all $P < 0.05$, Fig. 3A, B). Western blotting analysis further confirmed elevated protein levels of SULF1, COL1A1, FN1, α-SMA, and DESMIN following 48 h of TGF-β1 stimulation compared to the control group (Fig. 3C, $P < 0.05$). These findings indicate that human lung fibroblasts undergo increased expression of SULF1 during TGF-β1-induced myofibroblast differentiation, with HFL1 cells exhibiting higher levels of upregulation compared to MRC-5, thereby HFL1 was used for subsequent experiments.

SULF1 knockdown suppressed the activation and secretory capacity of lung fibroblasts

To investigate the impact of SULF1 on fibroblast activation and secretion capacity, we established a stably transfected cell line of HFL1 cells with SULF1 knockdown (sh-SULF1) and control cells (sh-NC) using lentiviral vectors. RT-qPCR analysis revealed that in both TGF-β1 stimulated and unstimulated conditions, expression levels of ACTA2, DESMIN, COL1A1, and FN1 were significantly lower in the sh-SULF1 group compared to the Blank or sh-NC group ($P < 0.05$) (Fig. 4A, B). Similarly, at the protein level, α-SMA, DESMIN, COL1A1, and FN1 were markedly reduced in the sh-SULF1 group under both TGF-β1 stimulated

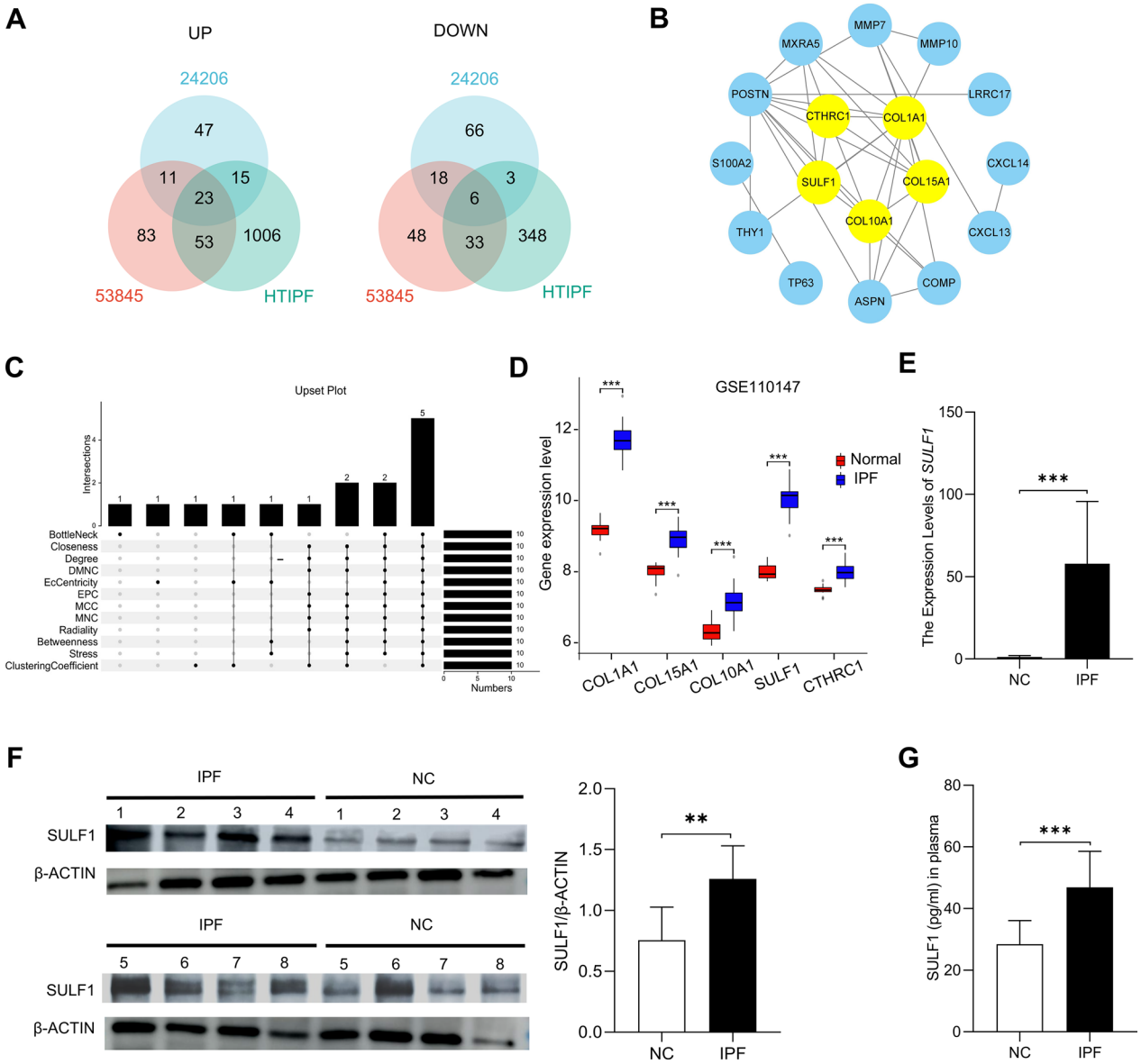

Fig. 1 SULF1 was upregulated in IPF. **A** The up-regulated genes of 3 datasets (HIPF, GSE24206, and GSE53845) showed an overlap of 23 differentially expressed genes (DEGs). The down-regulated genes of 3 datasets showed an overlap of 6 DEGs. **B** 17 genes were identified as hub genes by the MCODE plugin of Cytoscape. **C** The UpSet plot revealed an overlap of 5 hub genes among the top 10 genes identified by 12 topological methods (BottleNeck, Closeness, Degree, DMNC, EcCentricity, EPC, MCC, MNC, Radiality, Betweenness, Stress, ClusteringCoefficient) in CytoHubba plugin of Cytoscape. **D** Validate the elevated expression of the 5 hub genes in lung tissues of IPF patients (n = 22) compared to normal controls (n = 11) in GSE110147. **E** mRNA levels of SULF1 in lung tissue of IPF patients (n = 8) and normal control patients (n = 8) were determined by RT-qPCR, and β-ACTIN was used as an internal reference control. **F** Protein levels of SULF1 in lung tissue of IPF patients (n = 8) and normal control patients (n = 8) were determined by Western blotting, β-ACTIN was used as loading control. **G** The concentration of SULF1 in the plasma of IPF patients (n = 20) and normal control patients (n = 20) were determined by ELISA. Statistical analysis was conducted using Student's t-tests (*P < 0.05, **P < 0.01, ***P < 0.001)

and unstimulated conditions compared to the Blank or sh-NC group (P < 0.05) (Fig. 4C, D) as well. These findings indicate that SULF1 knockdown suppresses the activation and secretion capacity of lung fibroblasts, whether driven by TGF-β1 or not.

SULF1 knockdown suppressed the proliferation, migration, and invasion capability of lung fibroblasts

We further investigated the impact of SULF1 on the biological behaviors of lung fibroblasts. The CCK-8 assay demonstrated that, without TGF-β1 stimulation,

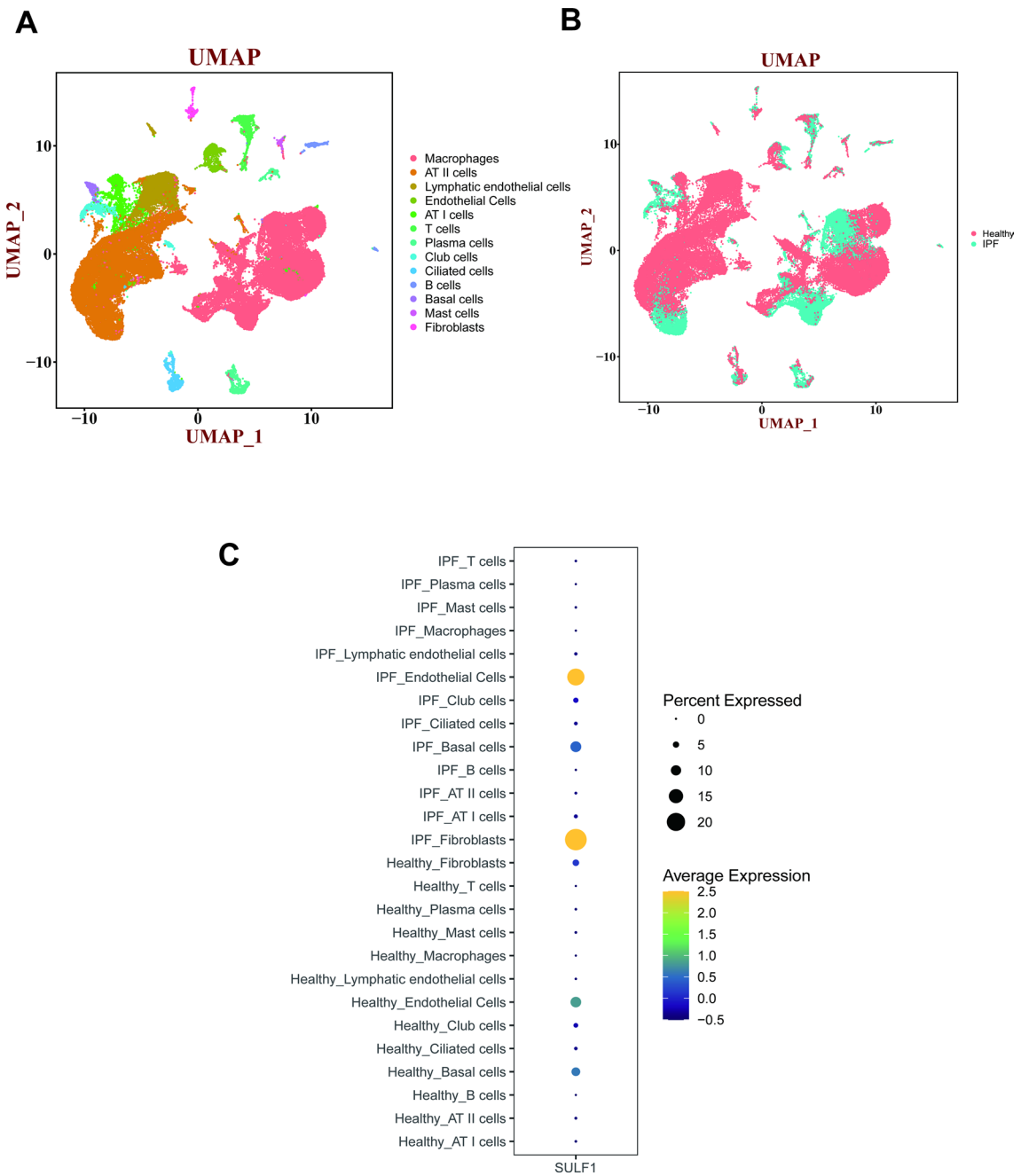

Fig. 2 SULF1 was upregulated mainly in human lung fibroblasts. **A** UMAP plot showed the different cell clusters of IPF patients and healthy controls in GSE122960. **B** UMAP plot showed the distribution of cells of IPF patients and healthy controls in different clusters. **C** The expression levels of SULF1 across different cell clusters

the proliferation rate significantly decreased in the sh-SULF1 group compared to the Blank or sh-NC groups (Fig. 5A, $P < 0.001$). Under TGF-β1 stimulation, both Blank + TGF-β1 and sh-NC + TGF-β1 groups showed a marked increase in proliferation compared to the Blank group (Fig. 5A, $P < 0.001$), whereas the sh-SULF1 + TGF-β1 group exhibited a significant decrease in proliferation compared to the Blank + TGF-β1 or sh-NC + TGF-β1 group (Fig. 5A, $P < 0.001$). Additionally, compared to the Blank group, the sh-SULF1 + TGF-β1 group also displayed a notable reduction in proliferation (Fig. 5A, $P < 0.001$). EdU assay results indicated a significant reduction in EdU-positive (EdU+) cells in the sh-SULF1 group compared

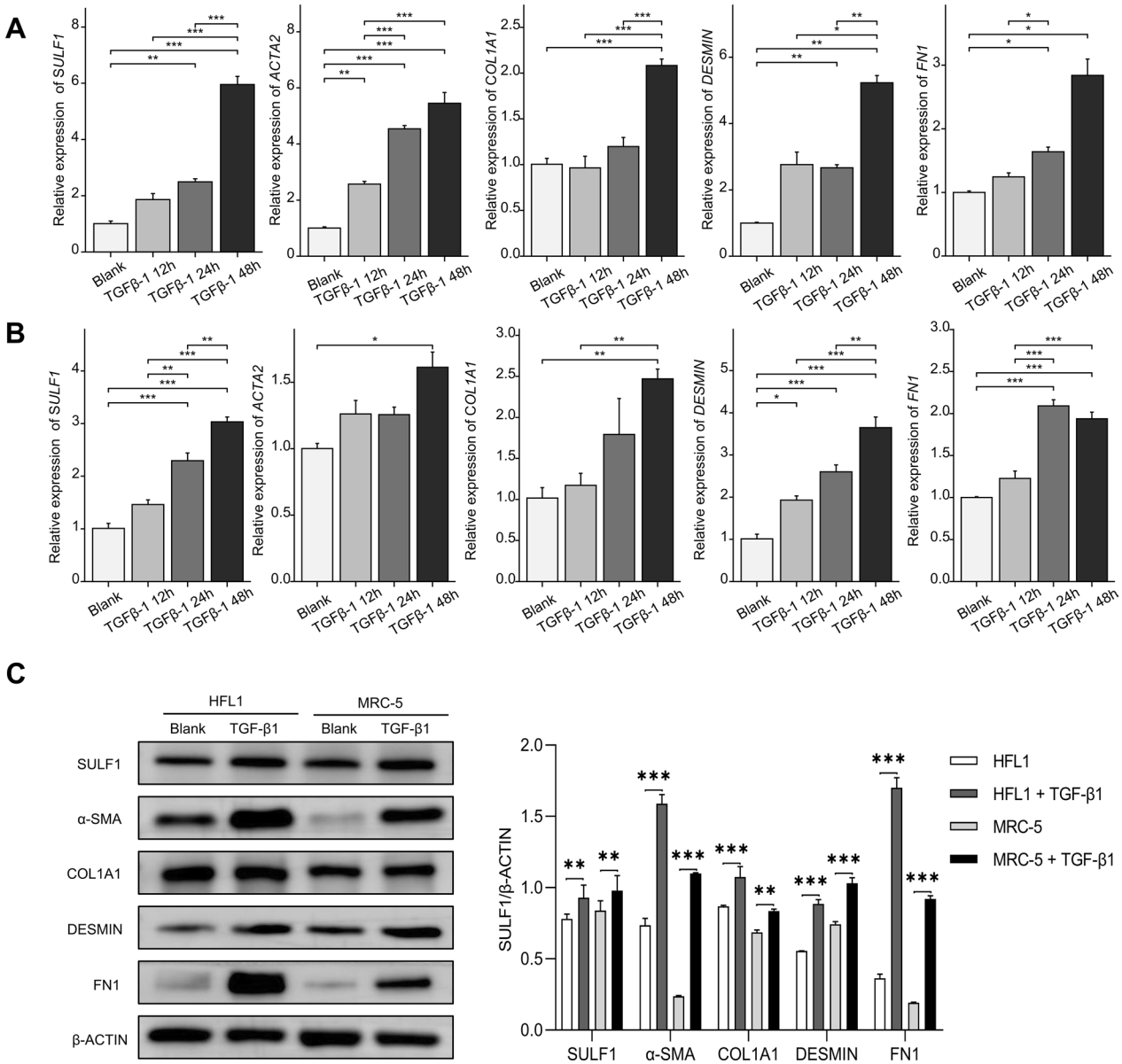

Fig. 3 Under stimulation by TGF-β1, fibroblasts exhibit increased secretion and activation capacity, accompanied by elevated expression of SULF1. **A** mRNA levels of SULF1, ACTA2, COL1A1, DESMIN, and FN1 in HFL1 cells were determined by RT-qPCR after stimulation with TGF-β1 for 12, 24, and 48 h, with β-ACTIN used as an internal reference control. **B** mRNA levels of SULF1, ACTA2, COL1A1, DESMIN, and FN1 in MRC-5 cells were determined by RT-qPCR after stimulation by TGF-β1 at 12, 24, and 48 h, β-ACTIN was used as internal reference control. **C** Protein levels of SULF1, α-SMA, COL1A1, DESMIN, and FN1 in HFL1 and MRC-5 cells were determined by Western blotting after stimulation with TGF-β1 for 48 h, and β-ACTIN was used as the loading control. Statistics for RT-qPCR were calculated using one-way ANOVA (*P < 0.05, **P < 0.01, ***P < 0.001). Statistics for Western blotting were calculated using Student's t-tests (*P < 0.05, **P < 0.01, ***P < 0.001)

to the Blank or sh-NC group (Fig. 5B, P < 0.001). Under TGF-β1 stimulation, both Blank + TGF-β1 and sh-NC + TGF-β1 groups showed a substantial increase in EdU^+ cells compared to the Blank group (Fig. 5B, P < 0.001), whereas the sh-SULF1 + TGF-β1 group displayed a significant decrease in EdU^+ cells compared to the Blank + TGF-β1 or sh-NC + TGF-β1 group (Fig. 5B, P < 0.001). Moreover, compared to the Blank group, the sh-SULF1 + TGF-β1 group also exhibited a notable decrease in EdU^+ cells (Fig. 5B, P < 0.05). These results indicate that knockdown of SULF1 inhibits the proliferative capacity of lung fibroblasts driven by TGF-β1 or not. Wound-healing assay revealed that, without TGF-β1 stimulation, the sh-SULF1 group exhibited

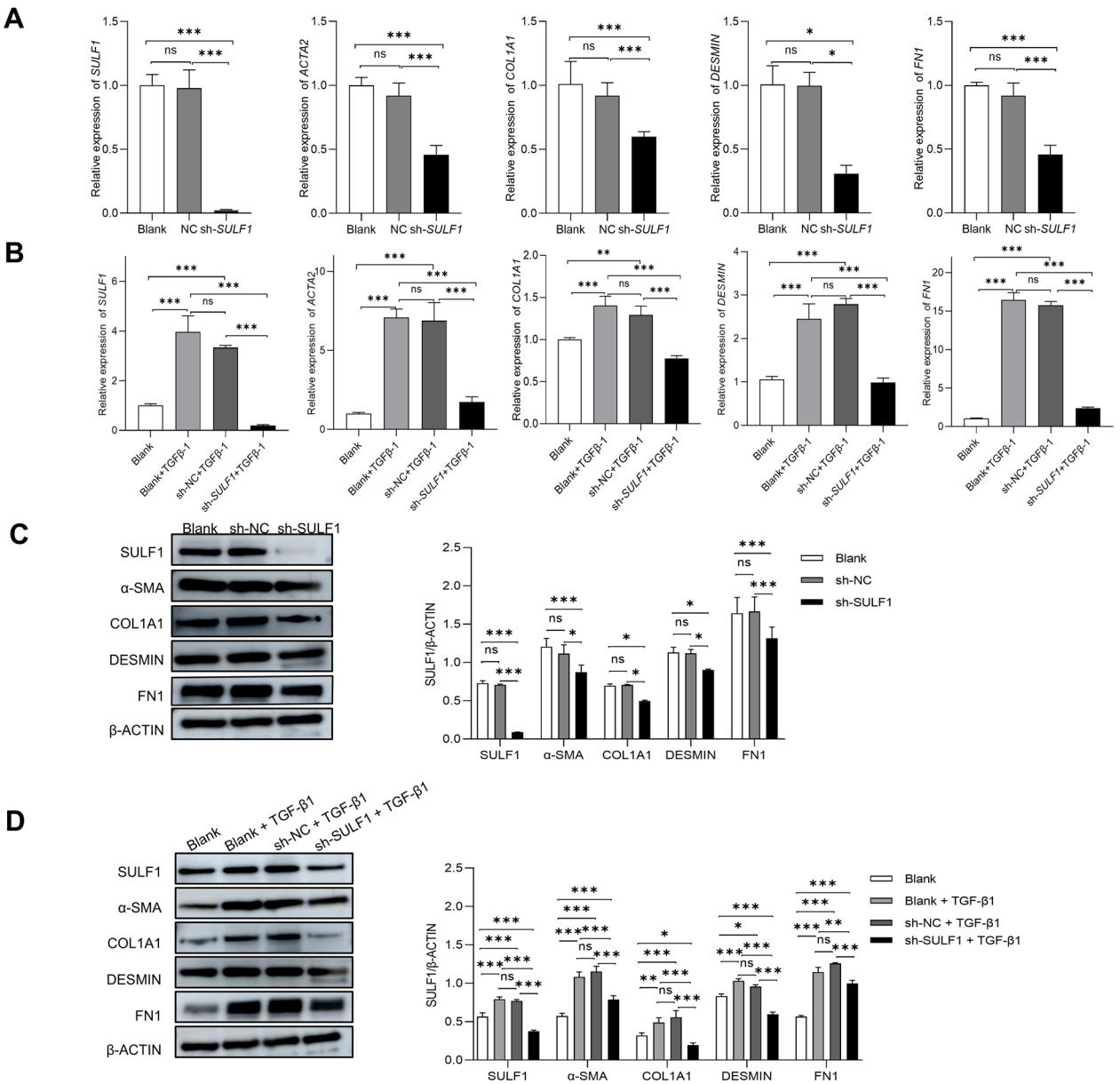

Fig. 4 SULF1 knockdown suppressed the proliferation, migration, and invasive capability of lung fibroblasts. **A** mRNA levels of SULF1, ACTA2, COL1A1, DESMIN, and FN1 in Blank, sh-NC, and sh-SULF1 HFL1 cells were determined by RT-qPCR, with β-ACTIN used as an internal reference control. **B** mRNA levels of SULF1, ACTA2, COL1A1, DESMIN, and FN1 in Blank HFL1 cells and Blank, sh-NC, and sh-SULF1 HFL1 cells were determined by RT-qPCR after stimulation by TGF-β1 at 48 h, with β-ACTIN used as an internal reference control. **C** Protein levels of SULF1, α-SMA, COL1A1, DESMIN, and FN1 in Blank, sh-NC, and sh-SULF1 HFL1 cells were determined by western blotting, β-ACTIN was used as the loading control. **D** Protein levels of SULF1, α-SMA, COL1A1, DESMIN, and FN1 in Blank HFL1 cells and Blank, sh-NC, and sh-SULF1 HFL1 cells were determined by western blotting after stimulation with TGF-β1 for 48 h, β-ACTIN was used as the loading control. Statistics were calculated using one-way ANOVA (*P < 0.05, **P < 0.01, ***P < 0.001)

a significant decrease in wound closure rate compared to the Blank or sh-NC group (Fig. 5C, P < 0.001). Under TGF-β1 stimulation, both Blank + TGF-β1 and sh-NC + TGF-β1 groups showed a marked increase in wound healing rate compared to the Blank group (Fig. 5C, P < 0.001), whereas the sh-SULF1 + TGF-β1 group displayed a significant decrease in wound healing rate compared to both Blank + TGF-β1 and sh-NC + TGF-β1 groups (Fig. 5C, P < 0.001). Furthermore, compared to the Blank group, the sh-SULF1 + TGF-β1 group also showed a notable decrease in wound healing rate (Fig. 5C, P < 0.001). These

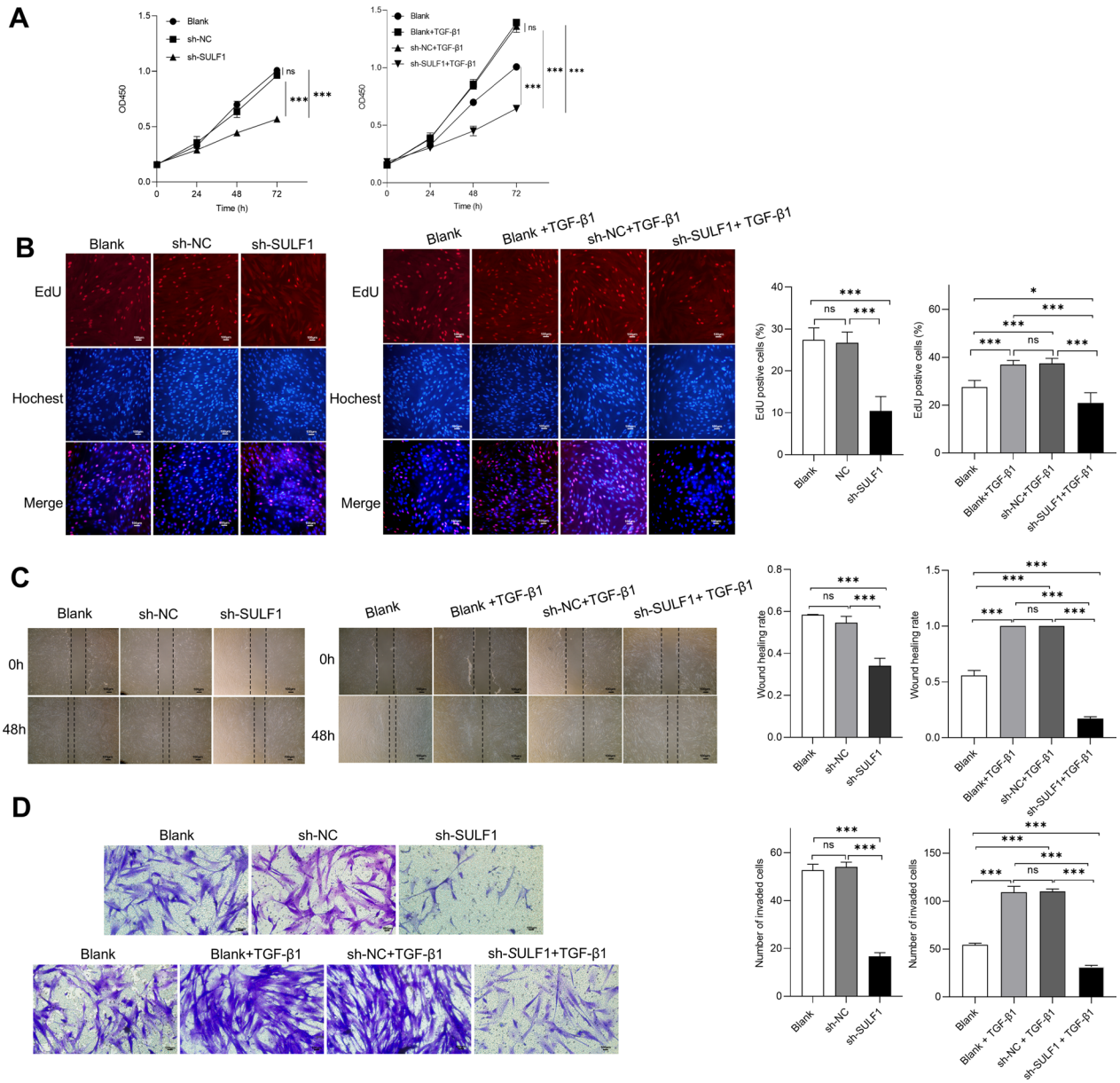

Fig. 5 SULF1 knockdown suppressed the proliferation, migration, and invasive capability of lung fibroblasts. **A** Cell proliferation of different groups was determined by CCK-8 assay. **B** Cell proliferation of different groups was determined by EdU assay. The histogram showed percentages of proliferative cells (EdU positive). The cell nuclei were stained blue with Hoechst 33342, while proliferating cells were labeled red with EdU. **C** Cell migration of different groups was determined by wound-healing assay. The histogram showed the percentage of wound closure area at 48 h post-scratching relative to the initial area. **D** Cell invasion of different groups was determined by transwell invasion assay. The histogram showed the number of invaded cells. Statistics for CCK-8 were calculated using two-way ANOVA (*P < 0.05, **P < 0.01, ***P < 0.001). Statistics for EdU assay, Wound-healing assay, and transwell invasion assay were calculated using one-way ANOVA (*P < 0.05, **P < 0.01, ***P < 0.001)

findings suggest that knockdown of SULF1 suppresses the migratory ability of lung fibroblasts driven by TGF-β1 or in its absence. Results from the transwell invasion assay indicated that, without TGF-β1 stimulation, the sh-SULF1 group displayed a significant reduction in the number of invaded cells compared to the Blank or sh-NC groups (Fig. 5D, $P < 0.001$). Under TGF-β1 stimulation, both Blank + TGF-β1 and sh-NC + TGF-β1 groups showed a notable increase in the number of invaded cells compared to the Blank group (Fig. 5D, $P < 0.001$), whereas the sh-SULF1 + TGF-β1 group exhibited a significant decrease in the number

of invaded cells compared to both Blank + TGF-β1 and sh-NC + TGF-β1 groups (Fig. 5D, $P < 0.001$). Additionally, compared to the Blank group, the sh-SULF1 + TGF-β1 group also demonstrated a marked decrease in the number of invaded cells (Fig. 5D, $P < 0.001$). Taken together, these results indicate that knockdown of SULF1 can inhibit the proliferation, migration, and invasion abilities of lung fibroblasts under both TGF-β1-driven and non-TGF-β1-driven conditions.

Mutual modulation of SULF1 and the TGF-β1/SMAD pathway

Under TGF-β1 stimulation, SULF1 expression in HFL1 cells was significantly reduced in the sh-SULF1 + TGF-β1 group compared to both the Blank + TGF-β1 and sh-NC + TGF-β1 groups (Fig. 6A, $P < 0.001$). Additionally,

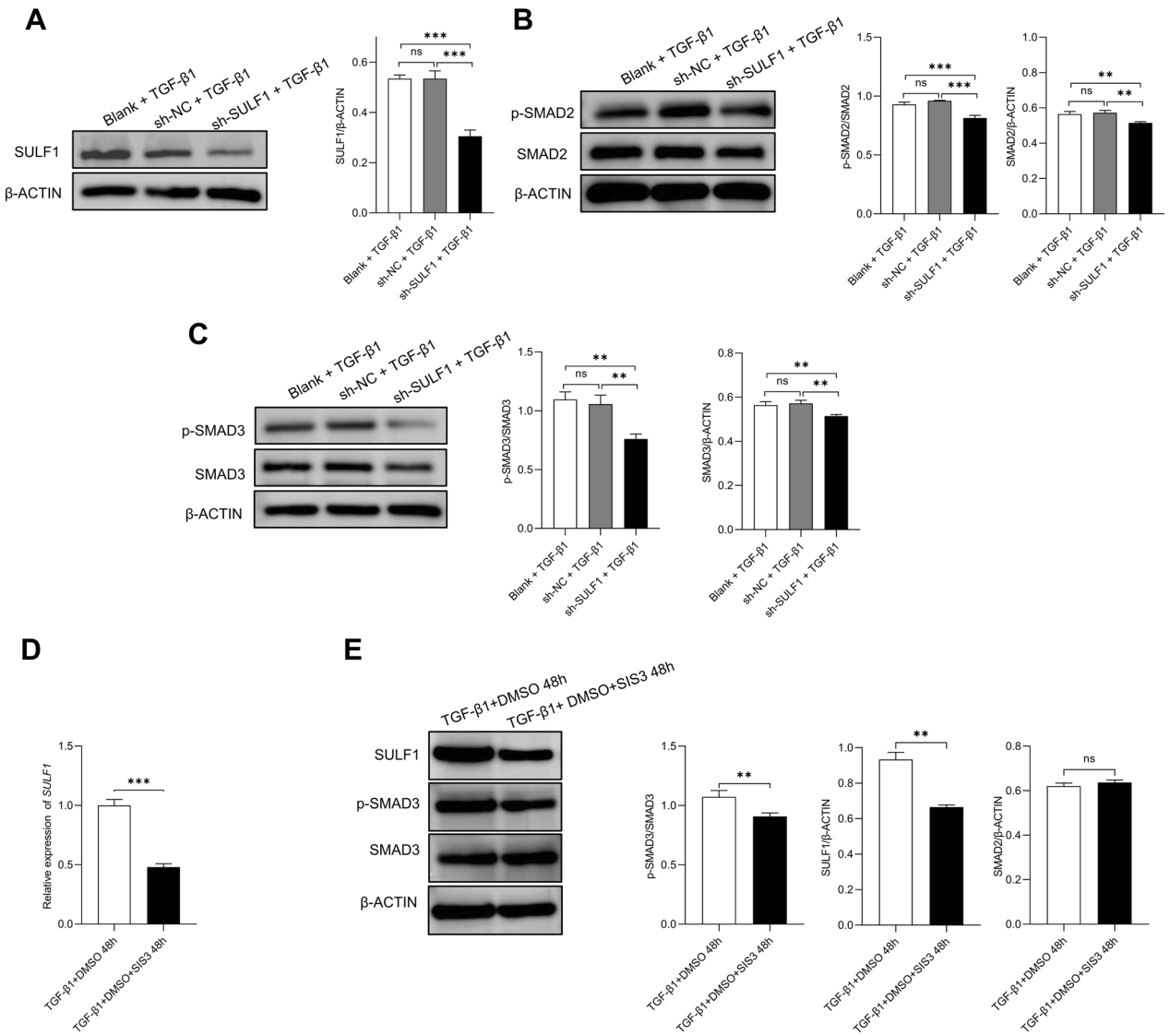

Fig. 6 **A** Protein levels of SULF1 in different groups were determined by western blotting after stimulation with TGF-β1 for 48 h, β-ACTIN was used as the loading control. **B** Protein levels of p-SMAD2, and SMAD2 in different groups were determined by western blotting after stimulation with TGF-β1 for 48 h, β-ACTIN was used as the loading control. **C** Protein levels of p-SMAD3, and SMAD3 in different groups were determined by western blotting after stimulation with TGF-β1 for 48 h, β-ACTIN was used as the loading control. **D** mRNA levels of SULF1 in different groups were determined by RT-qPCR after stimulation by TGF-β1 and SIS3 or TGF-β1 and DMSO at 48 h, with β-ACTIN used as an internal reference control. **E** Protein levels of SULF1, p-SMAD3, and SMAD3 in different groups were determined by western blotting after stimulation by TGF-β1 and SIS3 or TGF-β1 and DMSO at 48 h, β-ACTIN was used as the loading control. Statistics for western blotting were calculated using one-way ANOVA (*$P < 0.05$, **$P < 0.01$, ***$P < 0.001$). Statistics for RT-qPCR analysis were conducted using Student's t-tests (*$P < 0.05$, **$P < 0.01$, ***$P < 0.001$)

the levels of p-SMAD2/SMAD2 and p-SMAD3/SMAD3 were markedly decreased in the sh-SULF1 + TGF-β1 group compared to the Blank + TGF-β1 or sh-NC + TGF-β1 group (Fig. 6B, P < 0.01). Moreover, the expression levels of SMAD2 and SMAD3 were also significantly decreased in the sh-SULF1 + TGF-β1 group compared to the Blank + TGF-β1 or sh-NC + TGF-β1 groups (Fig. 6B, C, P < 0.01). These findings indicate that knockdown of SULF1 suppresses the TGF-β1/SMAD signaling pathway in HFL1 cells. Treatment of HFL1 cells with the SMAD3 phosphorylation inhibitor SIS3, we found that the ratio of pSMAD3 to total SMAD3 significantly decreased compared to the control group (P < 0.01, Fig. 6E). SIS3-treated HLF1 cells exhibited markedly reduced expression of SULF1 at both mRNA and protein levels compared to the control group (P < 0.01, Fig. 6D, E). Moreover, there was no significant difference in SMAD3 expression between the two groups (P > 0.05, Fig. 6E). These findings indicate that SIS3 suppresses activation of the TGF-β1/SMAD pathway and inhibits SULF1 expression. These results indicate that SULF1 and the TGFβ1/SMAD pathway mutually regulate each other. Furthermore, our experiments revealed that stimulation by TGFβ1 increases SULF1 expression, suggesting a potential positive feedback loop between SULF1 and the TGFβ1/SMAD pathway.

SULF1 promotes the release of TGF-β1 from TGFβRIII

TGFβRIII contains abundant heparan sulfate chains, which can bind and seal with TGF-β1. SULF1 selectively removes 6-O-sulfate groups from the heparan sulfate chains of TGFβRIII, releasing bound TGF-β1 and thereby activating downstream pathways potentially releasing bound TGF-β1. In this study, serum-free culture supernatants were collected over time, revealing an increasing concentration of TGF-β1 (Fig. 7A). sh-SULF1 HFL1 cells showed significantly reduced levels of TGF-β1 in the culture supernatant compared to both the Blank and sh-NC groups (Fig. 7A, P < 0.001). Co-IP experiments using an anti-TGFβRIII antibody demonstrated that TGFβRIII interacts with SULF1 and TGF-β1 (Fig. 7B). These findings suggest that SULF1 may catalyze the removal of 6-O-sulfate groups from the heparan sulfate chains of TGFβRIII, thereby releasing bound TGF-β1 and activating the downstream TGF-β1/SMAD signaling pathway.

Discussion

IPF is a chronic progressive lung disease with unclear pathogenesis, which hampers diagnostic and therapeutic research progress [18]. We conducted transcriptome sequencing on diseased lung tissues from IPF patients who underwent lung transplantation surgery and integrated our data with IPF lung tissue transcriptome datasets available in the GEO database. We aimed to elucidate potential pathogenic mechanisms underlying IPF. Ultimately, we found elevated expression of SULF1 in lung tissues of IPF patients compared to normal control lung tissues. We validated the elevated expression of SULF1 at both the transcriptional and protein levels in lung tissues from IPF patients. Moreover, previous studies have

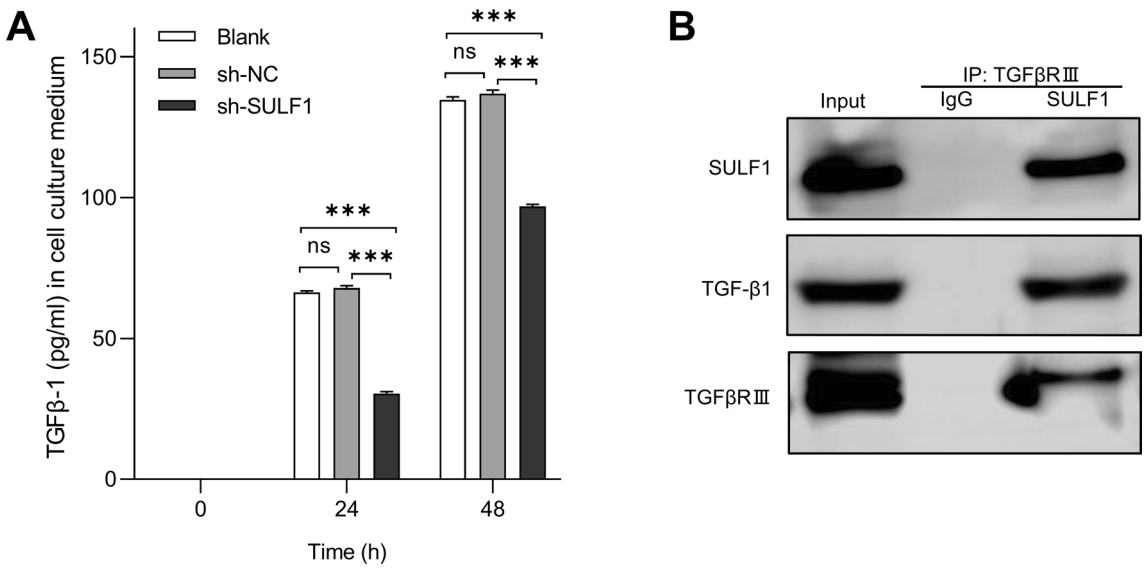

Fig. 7 **A** The concentration of TGF-β1 in the serum-free culture supernatants was determined by ELISA. Statistical analysis was conducted using Student's t-tests (*P < 0.05, **P < 0.01, ***P < 0.001). **B** The Co-IP with anti-TGFβRIII was performed and the precipitates were analyzed by western blotting with anti-SULF1 or anti-TGF-β1. IgG Co-IP was used as a negative control

demonstrated high expression of SULF1 in cardiac tissues of heart failure patients, where it plays a critical role in cardiac fibrosis [19]. These findings collectively support the notion that SULF1 may play a crucial role in the pathogenesis and progression of IPF.

Currently, IPF diagnosis relies on high-resolution CT and pathological recognition of UIP patterns, necessitating exclusion of other interstitial lung diseases or overlapping diseases [20]. Currently, the commonly used drugs pirfenidone and nintedanib have been shown to slow the decline in lung function and extend survival in patients with IPF [21, 22]. Early detection and accurate diagnosis of IPF are crucial for effective treatment [23]. However, early diagnosis of IPF still poses challenges at present. There are researches indicate that symptoms in patients with IPF often persist for over 5 years before a definitive diagnosis is established. Even when physicians detect Velcro crackles or clubbed fingers upon initial evaluation, fewer than 5% of patients receive a confirmed diagnosis within 1 year [24, 25]. Our study further revealed upregulated SULF1 concentration in plasma from IPF patients, proposing SULF1 as a potential peripheral blood biomarker for screening and diagnosis of IPF.

Through analysis of single-cell transcriptomic sequencing data from IPF lung tissues, we identified that SULF1 is predominantly expressed in lung fibroblasts. Fibroblasts are critical effector cells in the process of pulmonary fibrosis. When lung epithelial cells are damaged, fibroblasts become activated and can differentiate into myofibroblasts in an inflammatory environment. These cells contribute to ECM, collagen deposition, and secretion of pro-fibrotic factors, participating in the formation of pulmonary fibrosis [26]. Therefore, we chose pulmonary fibroblasts for subsequent experiments.

We demonstrate that TGF-β1, a key cytokine in fibrosis, induces SULF1 expression in human pulmonary fibroblasts, consistent with previous research [27]. Subsequently, we knocked down SULF1 in fibroblasts to investigate whether it could inhibit its various biological behaviors for fibrosis. We observed that downregulated SULF1 suppressed the activation and secretion capabilities of lung fibroblasts. This finding suggests that SULF1 plays a crucial role not only in regulating fibroblast activation but also potentially in modulating the fibrotic microenvironment in IPF.

Moreover, we found that SULF1 knockdown significantly reduces the proliferation, migration, and invasive capabilities of fibroblasts. These processes are fibroblast behaviors essential for fibrosis progression [6, 28]. It should be noted that even upon supplementation with recombinant human TGF-β1 during the culture of lung fibroblasts, the activation, secretion, proliferation, migration, and invasion of SULF1 knockdown cells were suppressed even compared to untreated normal control fibroblasts. It suggested SULF1 may modulate these processes via the TGF-β1/SMAD pathway.

Further investigation revealed that SULF1 knockdown reduces both the phosphorylation percentage and absolute levels of SMAD2 and SMAD3 in the downstream pathway of TGF-β1, indicating that SULF1 may play a critical regulatory role in the TGF-β1/SMAD pathway. In the TGF-β signaling pathway, SMAD2 and SMAD3 are known as receptor-regulated SMADs. This pathway also includes various other regulatory molecules, such as SMAD4, SMAD6, SMAD7, and SKI. SMAD4 can bind to the SMAD2/3 complex and subsequently translocate into the nucleus, where it directly or in conjunction with other regulators modulates the transcription of target genes [29, 30]. SMAD6 and SMAD7 act as inhibitory SMADs that prevent the activation of SMAD2 and SMAD3 and block the interaction between SMAD4 and the SMAD2/3 complex, thus providing negative regulation of the TGF-β pathway [29, 30]. SKI is a critical negative regulator of TGF-β signaling. It binds to SMAD2, SMAD3, and SMAD4, inhibiting SMAD proteins and ultimately suppressing TGF-β signal transduction [31]. In our current research, the impact of SULF1 on the expression of these factors has not yet been explored. SULF1 may regulate these molecules either directly or indirectly, influencing the expression of various fibrosis-related genes and thereby affecting the development of pulmonary fibrosis. Future studies will focus on investigating these molecules. Then, treatment with the SMAD3 phosphorylation inhibitor SIS3 suppresses the TGF-β1/SMAD pathway, resulting in a corresponding downregulation of SULF1 expression. This finding suggests a potential mutual regulation between SULF1 and the TGF-β1/SMAD pathway. TGF-β1 exerts its effects through three receptors: TGFβRI, TGFβRII, and TGFβRIII. Among these, TGFβRIII is uniquely an HSPG and a substrate for SULF1, but it does not activate downstream pathways, instead, it only sequesters TGF-β1 [32, 33]. There is a study that demonstrated that SULF1 catalyzes the release of TGF-β1 bound to TGFβRIII, activating downstream pathways to promote epithelial-mesenchymal transition in hepatocellular carcinoma cells, enhancing cancer cell migration and invasion [34]. Further experiments revealed a significant decrease in the concentration of TGF-β1 in the supernatant of sh-SULF1 group cultures compared to the sh-NC group. Co-IP experiment further confirmed the binding interaction between SULF1 and TGFβRIII. These findings collectively support that in lung fibroblasts, SULF1 can promote the release of TGF-β1 from TGF-βRIII and activate downstream pathways, thereby promoting fibrosis. Furthermore, our study indicates that fibroblasts exhibit increased SULF1

expression under stimulation by TGF-β1. Thus, this suggests a potential positive feedback loop between SULF1 and the TGF-β1/SMAD pathway, wherein SULF1 promotes the release of TGF-β1, and TGF-β1 subsequently further enhances SULF1 expression (Fig. 8).

Our study suggests that SULF1 may play a significant role in the pathogenesis of IPF, potentially paving the way for novel therapeutic approaches for IPF treatment. Inhibiting SULF1 may represent a novel intervention and therapeutic strategy for the prevention, treatment, and potential reversal of pulmonary fibrosis. Additionally, SULF1 holds promise as a peripheral blood biomarker for screening and diagnosis of IPF. Although our study has obtained important results, there are limitations we have to acknowledge. Firstly, our experiments still require validation in vivo to assess the impact of SULF1 on pulmonary fibrosis. Moving forward, we plan to develop SULF1 gene knockout mouse models and establish a murine pulmonary fibrosis model to address this issue. Secondly, while we have identified elevated SULF1 expression in lung tissues and blood of IPF patients, we have not investigated its relationship with disease progression and prognosis in these patients. Therefore, a prospective study may be necessary to examine the correlation between plasma SULF1 levels and disease progression and survival in IPF patients. Thirdly, given that SULF1 is upregulated in IPF patients and blocking SULF1 could potentially offer a new direction for IPF therapy, we have only performed knockdown experiments of the SULF1 gene in fibroblasts and have not yet conducted overexpression studies. Therefore, further research should involve overexpressing SULF1 in fibroblasts to observe its impact on the fibrotic process. Fourthly, our preliminary findings indicate that TGF-β1 may increase SULF1 expression in fibroblasts through the TGF-β1/SMAD pathway. However, the specific molecules and mechanisms involved require further investigation for clarification.

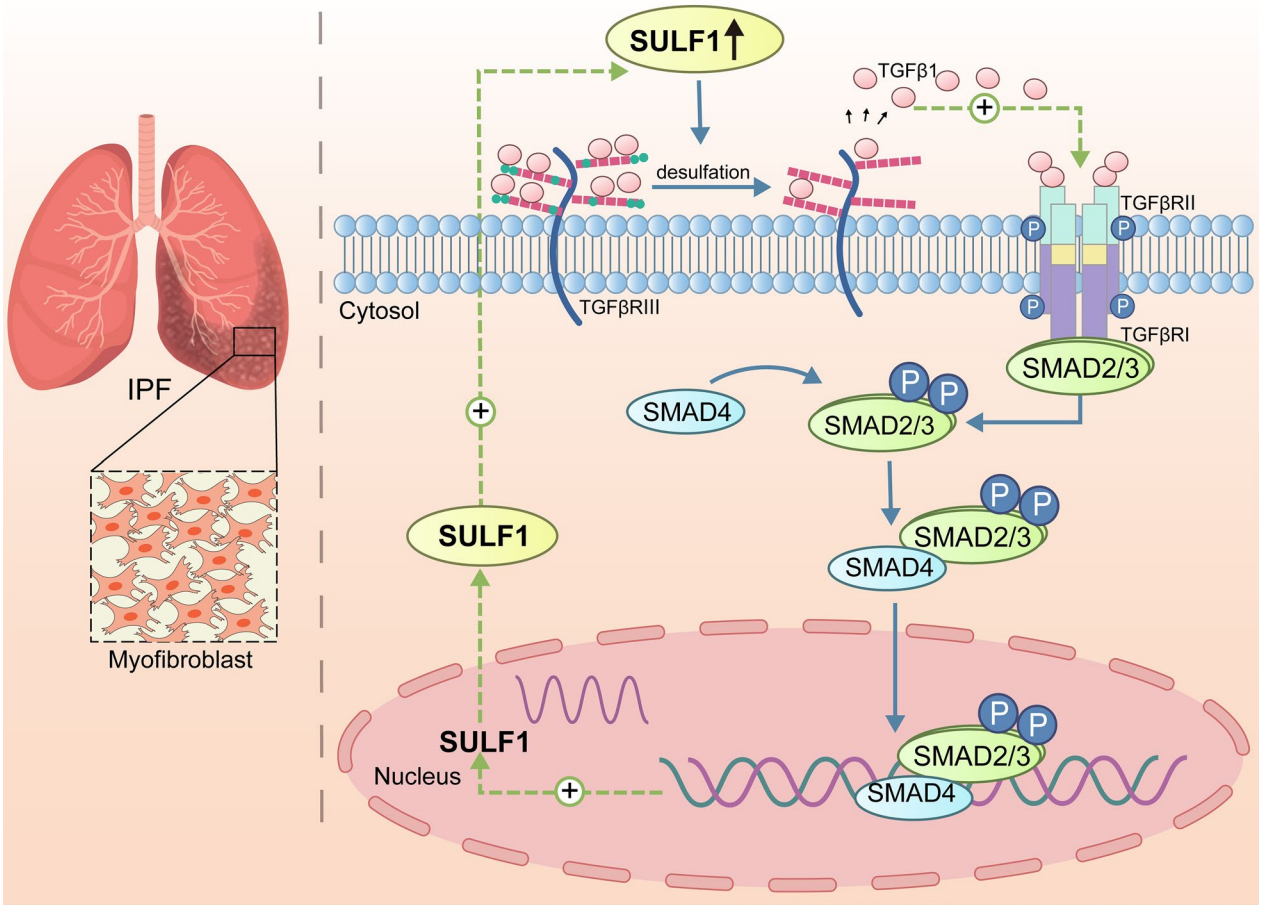

Fig. 8 Schema depicting proposed pro-fibrotic mechanisms of SULF1 in pulmonary fibrosis. SULF1 catalyzes the release of TGF-β1 bound to TGFβRIII, thereby activating the TGF-β1/SMAD pathway to promote fibrosis. Additionally, TGF-β1 induces SULF1 expression through the TGF-β1/SMAD pathway. There may be a potential positive feedback loop between SULF1 and the TGF-β1/SMAD pathway

Conclusions

In summary, our study reveals elevated SULF1 expression in lung tissues and plasma of IPF patients compared to the control. SULF1 can catalyze the release of TGF-β1 from TGFβRIII, thereby activating the TGF-β1/SMAD pathway to promote the progression of pulmonary fibrosis. Targeting SULF1 may offer a promising therapeutic strategy against IPF.

Abbreviations

CCK-8	Cell counting kit-8
Co-IP	Co-immunoprecipitation
DEGs	Differentially expressed genes
ECM	Extracellular matrix
EdU	5-Ethynyl-2′-deoxyuridine
Elisa	Enzyme-Linked Immunosorbent Assay
FC	Fold change
HSPGs	Heparan sulfate proteoglycans
ILD	Interstitial lung disease
IPF	Idiopathic pulmonary fibrosis
MCODE	Molecular complex detection
PCA	Principal Component Analysis
PPI	Protein–protein interaction
RT-qPCR	RNA extraction and Real-time quantitative reverse transcription PCR

Supplementary Information

The online version contains supplementary material available at https://doi.org/10.1186/s12967-024-05698-3.

Supplementary Material 1.

Acknowledgements

We acknowledge assistance with the access of analytic instruments from Translational Medicine Center at The First Affiliated Hospital of Zhengzhou University. Thanks for the Gene Expression Omnibus (GEO) database, which made the data available.

Author contributions

Concept and study design: Meng Tu, Chunya Lu, Ming Yang, Guojun Zhang. Experimental studies: Meng Tu, Yan Wang, Jing Li, Jiuling Cheng. Data analysis: Meng Tu, Hongxia Jia, Shanshan Chen, Ming Yang. Manuscript text: Meng Tu, Chunya Lu, Guojun Zhang. Manuscript editing: Meng Tu, Ming Yang, Guojun Zhang. All authors reviewed the manuscript.

Funding

This work was funded by Henan Key Laboratory of Interstitial Lung Diseases and Lung Transplantation.

Data availability

All datasets used and/or analyzed supporting the conclusions are available from the corresponding author upon reasonable request.

Declarations

Ethics approval and consent to participate

All methods performed in this study were carried out in accordance with the Declaration of Helsinki. This study was approved by Ethics Committee of the First Affiliated Hospital of Zhengzhou University (Ethics approval number: 2021-KY-0301). The studies were conducted in accordance with the local legislation and institutional requirements. The participants provided their written informed consent to participate in this study.

Consent for publication

All authors have approved the publication of this manuscript.

Competing interests

The authors declare no competing interests.

Author details

[1]Department of Respiratory Medicine, The First Affiliated Hospital of Zhengzhou University, Zhengzhou, Henan, China. [2]Henan Key Laboratory of Interstitial Lung Diseases and Lung Transplantation, Zhengzhou, Henan, China. [3]Priority Research Centre for Healthy Lungs, School of Biomedical Sciences and Pharmacy, Faculty of Health and Hunter Medical Research Institute, University of Newcastle, Callaghan, Australia. [4]Academy of Medical Sciences and Department of Immunology, College of Basic Medical Sciences, Zhengzhou University, Zhengzhou, Henan, China.

Received: 6 August 2024 Accepted: 22 September 2024
Published online: 01 October 2024

References

1. Raghu G, Remy-Jardin M, Myers JL, Richeldi L, Ryerson CJ, Lederer DJ, et al. Diagnosis of idiopathic pulmonary fibrosis. An Official ATS/ERS/JRS/ALAT clinical practice guideline. Am J Respir Crit Care Med. 2018;198(5):e44–68.
2. Munchel JK, Shea BS. Diagnosis and management of idiopathic pulmonary fibrosis. R I Med J. 2021;104(7):26–9.
3. Maher TM, Bendstrup E, Dron L, Langley J, Smith G, Khalid JM, et al. Global incidence and prevalence of idiopathic pulmonary fibrosis. Respir Res. 2021;22(1):197.
4. Hopkins RB, Burke N, Fell C, Dion G, Kolb M. Epidemiology and survival of idiopathic pulmonary fibrosis from national data in Canada. Eur Respir J. 2016;48(1):187–95.
5. Cai M, Zhu M, Ban C, Su J, Ye Q, Liu Y, et al. Clinical features and outcomes of 210 patients with idiopathic pulmonary fibrosis. Chin Med J. 2014;127(10):1868–73.
6. Moss BJ, Ryter SW, Rosas IO. Pathogenic mechanisms underlying idiopathic pulmonary fibrosis. Annu Rev Pathol. 2022;17:515–46.
7. Schafer MJ, White TA, Iijima K, Haak AJ, Ligresti G, Atkinson EJ, et al. Cellular senescence mediates fibrotic pulmonary disease. Nat Commun. 2017;8:14532.
8. O'Dwyer DN, Ashley SL, Gurczynski SJ, Xia M, Wilke C, Falkowski NR, et al. Lung microbiota contribute to pulmonary inflammation and disease progression in pulmonary fibrosis. Am J Respir Crit Care Med. 2019;199(9):1127–38.
9. Noble PW, Albera C, Bradford WZ, Costabel U, du Bois RM, Fagan EA, et al. Pirfenidone for idiopathic pulmonary fibrosis: analysis of pooled data from three multinational phase 3 trials. Eur Respir J. 2016;47(1):243–53.
10. Brown KK, Flaherty KR, Cottin V, Raghu G, Inoue Y, Azuma A, et al. Lung function outcomes in the INPULSIS((R)) trials of nintedanib in idiopathic pulmonary fibrosis. Respir Med. 2019;146:42–8.
11. Mackintosh JA, Keir G, Troy LK, Holland AE, Grainge C, Chambers DC, et al. Treatment of idiopathic pulmonary fibrosis and progressive pulmonary fibrosis: a position statement from the Thoracic Society of Australia and New Zealand 2023 revision. Respirology. 2024;29(2):105–35.
12. Vancheri C, Failla M, Crimi N, Raghu G. Idiopathic pulmonary fibrosis: a disease with similarities and links to cancer biology. Eur Respir J. 2010;35(3):496–504.
13. Pascale RM, Calvisi DF, Feo F. Sulfatase 1: a new Jekyll and Hyde in hepatocellular carcinoma? Transl Gastroenterol Hepatol. 2016;1:43.
14. El Masri R, Seffouh A, Lortat-Jacob H, Vives RR. The "in and out" of glucosamine 6-O-sulfation: the 6th sense of heparan sulfate. Glycoconj J. 2017;34(3):285–98.
15. Yang JD, Sun Z, Hu C, Lai J, Dove R, Nakamura I, et al. Sulfatase 1 and sulfatase 2 in hepatocellular carcinoma: associated signaling pathways, tumor phenotypes, and survival. Genes Chromosomes Cancer. 2011;50(2):122–35.
16. Phan THG, Paliogiannis P, Nasrallah GK, Giordo R, Eid AH, Fois AG, et al. Emerging cellular and molecular determinants of idiopathic pulmonary fibrosis. Cell Mol Life Sci. 2021;78(5):2031–57.
17. Wollin L, Wex E, Pautsch A, Schnapp G, Hostettler KE, Stowasser S, et al. Mode of action of nintedanib in the treatment of idiopathic pulmonary fibrosis. Eur Respir J. 2015;45(5):1434–45.

18. Wang Q, Xie Z, Wan N, Yang L, Jin Z, Jin F, et al. Potential biomarkers for diagnosis and disease evaluation of idiopathic pulmonary fibrosis. Chin Med J. 2023;136(11):1278–90.
19. Wu J, Subbaiah KCV, Xie LH, Jiang F, Khor ES, Mickelsen D, et al. Glutamyl-Prolyl-tRNA synthetase regulates proline-rich pro-fibrotic protein synthesis during cardiac fibrosis. Circ Res. 2020;127(6):827–46.
20. Bartold K, Iskierko Z, Sharma PS, Lin HY, Kutner W. Idiopathic pulmonary fibrosis (IPF): Diagnostic routes using novel biomarkers. Biomed J. 2024;47: 100729.
21. King TE Jr, Bradford WZ, Castro-Bernardini S, Fagan EA, Glaspole I, Glassberg MK, et al. A phase 3 trial of pirfenidone in patients with idiopathic pulmonary fibrosis. N Engl J Med. 2014;370(22):2083–92.
22. Richeldi L, du Bois RM, Raghu G, Azuma A, Brown KK, Costabel U, et al. Efficacy and safety of nintedanib in idiopathic pulmonary fibrosis. N Engl J Med. 2014;370(22):2071–82.
23. Martinez FJ, Collard HR, Pardo A, Raghu G, Richeldi L, Selman M, et al. Idiopathic pulmonary fibrosis. Nat Rev Dis Primers. 2017;3:17074.
24. Hewson T, McKeever TM, Gibson JE, Navaratnam V, Hubbard RB, Hutchinson JP. Timing of onset of symptoms in people with idiopathic pulmonary fibrosis. Thorax. 2017;73:683–5.
25. Thickett D, Voorham J, Ryan R, Jones R, Coker R, Wilson AM, et al. Historical database cohort study addressing the clinical patterns prior to idiopathic pulmonary fibrosis (IPF) diagnosis in UK primary care. BMJ Open. 2020;10(5): e034428.
26. Ma H, Wu X, Li Y, Xia Y. Research progress in the molecular mechanisms, therapeutic targets, and drug development of idiopathic pulmonary fibrosis. Front Pharmacol. 2022;13: 963054.
27. Yue X, Li X, Nguyen HT, Chin DR, Sullivan DE, Lasky JA. Transforming growth factor-beta1 induces heparan sulfate 6-O-endosulfatase 1 expression in vitro and in vivo. J Biol Chem. 2008;283(29):20397–407.
28. Liu G, Philp AM, Corte T, Travis MA, Schilter H, Hansbro NG, et al. Therapeutic targets in lung tissue remodelling and fibrosis. Pharmacol Ther. 2021;225: 107839.
29. Derynck R, Zhang YE. Smad-dependent and Smad-independent pathways in TGF-beta family signalling. Nature. 2003;425(6958):577–84.
30. Frangogiannis N. Transforming growth factor-beta in tissue fibrosis. J Exp Med. 2020;217(3): e20190103.
31. Deheuninck J, Luo K. Ski and SnoN, potent negative regulators of TGF-beta signaling. Cell Res. 2009;19(1):47–57.
32. Lopez-Casillas F, Wrana JL, Massague J. Betaglycan presents ligand to the TGF beta signaling receptor. Cell. 1993;73(7):1435–44.
33. Vilchis-Landeros MM, Montiel JL, Mendoza V, Mendoza-Hernandez G, Lopez-Casillas F. Recombinant soluble betaglycan is a potent and isoform-selective transforming growth factor-beta neutralizing agent. Biochem J. 2001;355(Pt 1):215–22.
34. Dhanasekaran R, Nakamura I, Hu C, Chen G, Oseini AM, Seven ES, et al. Activation of the transforming growth factor-beta/SMAD transcriptional pathway underlies a novel tumor-promoting role of sulfatase 1 in hepatocellular carcinoma. Hepatology. 2015;61(4):1269–83.

Publisher's Note